MODELING AND NUMERICAL SIMULATION OF AN ALGORITHM FOR THE INERTIAL SENSORS ERRORS REDUCTION AND FOR THE INCREASE OF THE STRAP-DOWN NAVIGATOR REDUNDANCY DEGREE IN A LOW COST ARCHITECTURE

Lucian T. Grigorie[1], Ruxandra M. Botez[2]
[1] *Department of Avionics, Faculty of Electrical Engineering, University of Craiova, Craiova, Dolj, Romania*
E-mail: lgrigore@elth.ucv.ro
[2] *Department of Automated Manufacturing Engineering, École de technologie supérieure, Montreal, Quebec, Canada*
E-mail: Ruxandra.Botez@etsmtl.ca

Received August 2008, Accepted February 2010
No. 08-CSME-29, E.I.C. Accession 3067

ABSTRACT

In this paper, an algorithm for the inertial sensors errors reduction in a strap-down inertial navigation system, using several miniaturized inertial sensors for each axis of the vehicle frame, is conceived. The algorithm is based on the idea of the maximum ratio-combined telecommunications method. We consider that it would be much more advantageous to set a high number of miniaturized sensors on each input axis of the strap-down inertial system instead of a single one, more accurate but expensive and with larger dimensions. Moreover, a redundant system, which would isolate any of the sensors in case of its malfunctioning, is obtained. In order to test the algorithm, Simulink code is used for algorithm and for the acceleration inertial sensors modeling. The Simulink resulted sensors models include their real errors, based on the data sheets parameters, and were conceived based on the IEEE analytical standardized accelerometers model. An integration algorithm is obtained, in which the signal noise power delivered to the navigation processor, is reduced, proportionally with the number of the integrated sensors. At the same time, the bias of the resulted signal is reduced, and provides a high redundancy degree for the strap-down inertial navigation system at a lower cost than at the cost of more accurate and expensive sensors.

MODÉLISATION ET SIMULATION NUMÉRIQUE D'UN ALGORITHME POUR LA RÉDUCTION DES ERREURS DES CAPTEURS INERTIELS ET DE L'AUGMENTATION DU DEGRÉ DE REDONDANCE D'UN NAVIGATEUR INERTIEL À COMPOSANTES LIÉES DANS UNE ARCHITECTURE À FAIBLE COÛT

RÉSUMÉ

Un algorithme est conçu pour réduire les erreurs des capteurs inertiels dans un navigateur inertiel à composantes liées en utilisant plusieurs capteurs sur chacun des trois axes du système. Pour tester l'algorithme, le code Simulink a été utilisé pour modéliser les capteurs inertiels. Les modèles de ces capteurs incluent les erreurs réelles des capteurs utilisés, en se basant sur des paramètres fournis par les fiches techniques. De plus, l'algorithme est conçu en Simulink, et il est testé en utilisant le modèle des capteurs d'accélération. Les résultats des simulations numériques confirment l'obtention d'un algorithme d'intégration pour les capteurs inertiels en miniature, basé sur la mise sur le même axe de plusieurs capteurs de même type. La puissance du bruit du signal rendu au processeur de navigation est réduite, proportionnellement avec le nombre des capteurs intégrés. L'algorithme réduit le biais du signal résultant et fournit un degré élevé de redondance pour le navigateur inertiel à composantes liées à un faible coût par rapport au coût des capteurs plus précis et coûteux.

NOMENCLATURE

E	the sensor output
K, K_1	the scale factor
K_o, B	the bias
K_2, K_3	second-order, respectively third-order, nonlinearity coefficients
K_{ip}, K_{io}	cross-coupling coefficients
N	the misalignment of the sensitive axis
a	the output acceleration (perturbed signal)
a_c	the cross-axis acceleration
a_i, a_p, a_o	the applied acceleration components along the positive input, pendulous, and reference axes, respectively
a_{IA}	the acceleration obtained through the application of the integration algorithm
a_{sensors}	the output acceleration signal from the integrated system of sensors
a_s	the acceleration indicated by the accelerometer
$\bar{c}_i$	the average of m consecutive samples acquired from the accelerometer i
c_{ij}	the reading no. j, perturbed, from the i sensor on the input axis
$c_{i(m+1)}$	the reading no. m+1 from the sensor i
c_{m+1}	the quantity read by the integrated system of n sensors after m+1 steps of signal acquisitions from the sensors
g	the acceleration of gravity
i	the sensors index
j	the readings index
k_c	the cross-axis sensitivity
m	the number of the samples considered for the calculation of the standard deviation
n	the number of the sensors
$p(i)$	the weight of the i accelerometer
ΔK	the scale factor calibration error
δ_o, δ_p	misalignments of the input axis with respect to the input reference axis about the output reference and pendulous reference axes, respectively
v	the sensor noise
v_d	the noise density
σ_i	the standard deviation of the readings
σ_i^2	the dispersion of the readings

1. INTRODUCTION

Inertial navigation is a process in which the vehicle position is computed through the sum of the initial positions with the distances covered in known directions. The positioning errors result from the initial conditions imperfection, from the errors dues to the numerical calculations in the inertial system (truncation, commutation, etc.), and from the inertial sensors internal errors [1, 2].

In case when no compensation algorithm is used, perturbed accelerations and angular speeds are obtained from their vehicle dynamics accelerations and angular speeds dues to the internal errors of the inertial sensors, as shown on Fig. 1. Therefore, the inertial sensors performances (the minimum of internal errors) are very important for the navigation system precision, and should be considered in the system's design phase [3–5].

The aerospace industry tendencies to design and build unmanned aircraft (UAV), micro and nano-satellites, easy to launch in space which will have the performances analogous with the

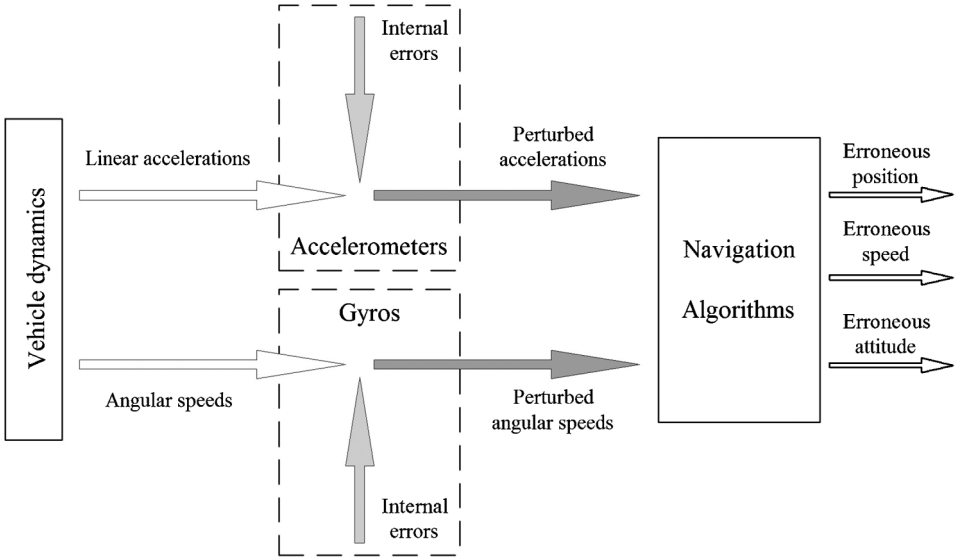

Fig. 1. The influence of the inertial sensors internal errors on the inertial navigator.

actual satellites, imposed a nimble rhythm to the expansion of various technologies. These technologies are: the nanotechnologies, the MEMS (Micro-Electro-Mechanical Sensors) and the MOEMS (Micro-Opto-Electro-Mechanical sensors) technologies in the inertial sensors field [6–9]. The use of such miniaturized sensors ensures the redundancy for the strap-down inertial navigation systems through the miscellaneous dedicated architectures [10, 11] and at low-costs with respect to the case of non-miniaturized and very precise inertial sensors use. These technologies allow the implementation of the entire inertial navigation system in a single chip, including here all sensors and circuits for the signals conditioning [7, 12].

From another point of view, the miniaturised sensors have disadvantages dues to the performances decrease with the miniaturization degree increase [2, 7]. They are quite noisy, because for most of the acceleration sensors with bandwidths between 100 Hz and 2500 Hz, the noise density is between 100 $\mu g/Hz^{1/2}$ and a few hundreds of $\mu g/Hz^{1/2}$. For gyro sensors with pass bandwidths between 50 Hz and 100 Hz, the noise density is between 0.0035 $(^\circ/s)/Hz^{1/2}$ and 0.1$(^\circ/s)/Hz^{1/2}$.

For the same category of miniaturised sensors, the noise density can vary from one sensor to another within 20% of the catalogue value [2, 6, 7, 13–17]. The noise filtering is not recommended because it could alter the useful signal (located in the 0 Hz÷100 Hz interval), therefore the sensor output would not reflect exactly the input signal [1, 2, 18–21]. The bias value stability, the scale factor calibration, the cross-axis sensitivity for the accelerometers and the sensitivity at the accelerations applied along any gyros given axis are negative influenced, for example by the noise increase [1, 3]. For all these parameters, the miniaturised sensors data sheets stipulate maximum relatively high values, without specifying exactly their values to be corrected [6, 13–17].

It is known that for miniaturised inertial sensors: the bias, the scale factor calibration error and the sensitivity at the accelerations may take random values in an interval, which is obtained from the sensor technical characteristics, and the sensors noise is randomly generated, with its density ranging from 80% of the maximum value provided by the data sheets and that maximum value. For all these reasons, an algorithm for the perturbations reduction is here conceived and shown. This algorithm is based on the maximal ratio-

combining method from telecommunications area [22–24]; it is the first time when such an algorithm idea is used for inertial navigation. Thus, we considered that it would be less expensive, from both weights and costs points of view, to set a high number of miniaturised sensors on each input axis of the strap-down inertial system. These sensors are cheaper and noisier with respect to an expensive sensor, which would be more accurate but with larger dimensions. Moreover, if the algorithm of integration of the n sensors mounted on an axis would be correctly elaborated, one can obtain a redundant system, which would isolate any of the n sensors in case of its malfunctioning.

2. SENSORS' INTEGRATION ALGORITHM

The inertial navigation principle consists in the detection of the vehicle linear acceleration and angular speeds components in its tri-axial reference frame, followed by their processing using the navigation algorithm with the aim to obtain the vehicle positions, speeds and attitudes (see Fig. 1). In this way, our idea is to use n miniaturised sensors of acceleration or angular speed for each vehicle frame axis.

The proposed algorithm integrates all the n acceleration or angular speed sensors fixed on the same axis. This algorithm is based on the idea that for the determination of acceleration or angular speed components on the considered axis, each sensor should have a weight inverse proportionally with the standard deviation of the last m samples acquired from it [3] (Fig. 2). For redundancy achievement, in the case of malfunctioning or breaking-down of one or more sensors on that axis, they are given null weights and are excluded from calculation.

Considering c_{ij} as the perturbed j^{th} reading, from the i^{th} sensor on the input axis, the average of m consecutive samples acquired from the i^{th} accelerometer is:

$$\bar{c}_i = \frac{1}{m}\sum_{j=1}^{m} c_{ij}, \tag{1}$$

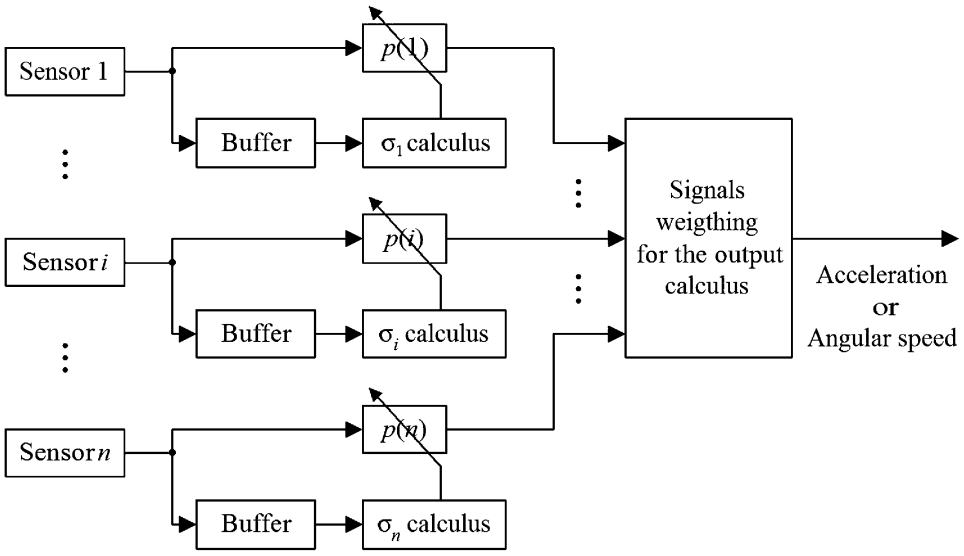

Fig. 2. Sensors' integration algorithm scheme.

and the dispersion of the readings is:

$$\sigma_i^2 = \frac{1}{m}\sum_{j=1}^{m}(c_{ij} - \bar{c}_i)^2. \tag{2}$$

For each sensor, the larger is the weight $p(i)$, the smaller is the standard deviation σ_i. Considering $c_{i(m+1)}$ as the reading no. $m + 1$ from the i^{th} sensor, the quantity read by the integrated system of n sensors following $m + 1$ steps of signal acquisitions from them is:

$$c_{m+1} = \left(\sum_{i=1}^{n} p_i \cdot c_{i\,(m+1)}\right) / \left(\sum_{i=1}^{n} p_i\right). \tag{3}$$

We denote the sum of the n accelerometers' weights by:

$$\sum_{i=1}^{n} p_i = 1 \tag{4}$$

The inverse proportionality between weight p_i and the standard deviation σ_i is:

$$\sigma_1 \cdot p_1 = \sigma_2 \cdot p_2 = \ldots = \sigma_n \cdot p_n, \tag{5}$$

Then, we obtain:

$$p_i = (1/\sigma_i) \cdot \left(1 / \sum_{k=1}^{n} (1/\sigma_k)\right). \tag{6}$$

The output quantity for the $m + 1^{\text{th}}$ sample is:

$$c_{m+1} = \frac{\sum_{i=1}^{n} (c_{i\,(m+1)}/\sigma_i)}{\sum_{k=1}^{n} (1/\sigma_k)}, \tag{7}$$

$$c_{m+1} = \frac{1}{\sum_{k=1}^{n} \frac{1}{\sqrt{\sum_{j=1}^{m} (c_{kj} - \bar{c}_k)^2}}} \cdot \sum_{i=1}^{n} \frac{c_{i\,(m+1)}}{\sqrt{\sum_{j=1}^{m} (c_{ij} - \bar{c}_i)^2}}. \tag{8}$$

If one of the sensors breaks down, the standard deviation is null or has very large values. When Eq. (8) is implemented into the software, the zero value can be conditioned for the malfunctioning sensor weights, if its corresponding standard deviation is null. The same weights will be given to it, if the standard deviation exceeds a maximum limit.

Based on the previously presented algorithm shown in Fig. 2, and in Eqs. (1)–(8), a Matlab/Simulink model is conceived (Fig. 3). The behaviour of the sensors integrated system would be simulated for any number of sensors mounted on the input axis. In order to well simulate the algorithm model behaviour close to real conditions, perturbed signals should be applied to its inputs. In this way, an error model for the inertial sensors should also be conceived.

The signals provided by the n sensors set on the same axis are applied at the model algorithm inputs using the multiplexing block "Mux" (Fig. 3). The "Buffer" block generates clusters of m successive samples from the sensors reading on each input channel of the multiplexer. For each calculation step, a new sample gets into the cluster and another sample goes out. Practically the "Buffer" has the structure of an $n \times m$ matrix, in which, for each calculation step, a column is an input at its left and another column is its output at its right. Using the "Standard Deviation" Simulink block, the standard deviation is calculated for each cluster of m successive samples on the n input channels. The "Switch" block is the one deciding if each of the n sensors has a good functioning. This block gives the zero values to the weights of malfunctioning sensors. Equation (6) is implemented in the model between the "Switch" and "Product" blocks for each of the n channels. The end of Eq. (8) implementations is done using the "Product" block (its inputs are read on the n^{th} channel at the sample $m + 1$ ($c_{i(m+1)}$), and they are the sensors weights), the "Matrix Sum1" and the "Frame Status Conversion" blocks. In the last two blocks, the sum of the weighted inputs $c_{i(m+1)}$, and the output quantity c_{m+1} numerical conversion, respectively are realized.

In order to evaluate the proposed algorithm, the Matlab/Simulink model was realized for the acceleration sensors. For this modelling, the sensors data sheets [6, 13–17] and the Institute of Electrical and Electronics Engineers (IEEE) equivalent accelerometer models [25–27] are used.

3. ACCELERATION SENSORS' MODEL

Based on the parameters and errors of the acceleration and rotation sensors, analytical models were realized and standardized by the IEEE specialists for different categories of inertial sensors [4]. The IEEE analytical models are used by the producers in the sensors calibration processes, to obtain their performances in a common language, through the data sheets. In addition, these models have a very important role in the compensation process of most of sensors errors.

3.1. The IEEE Accelerometers Analytical Model

From the IEEE standards corresponding to the accelerometers test procedures [25–27], the accelerometers model assumes the presence of errors dues to the bias, scale nonlinearity,

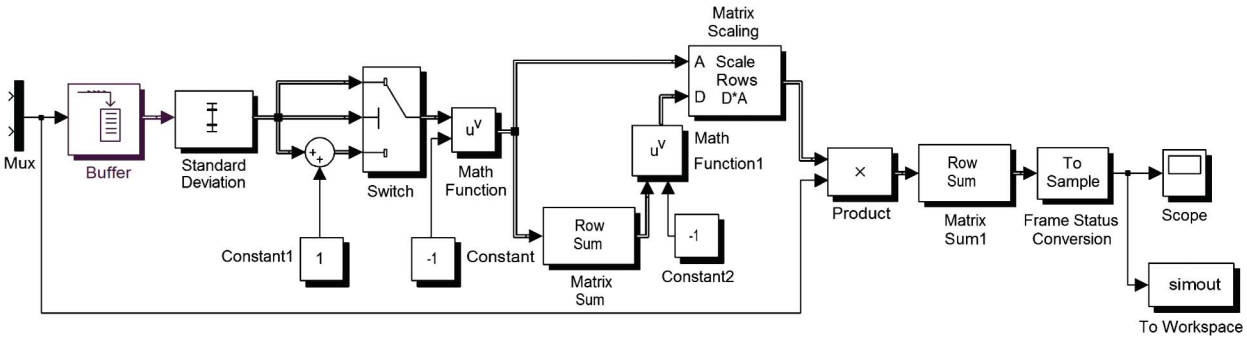

Fig. 3. The Matlab/Simulink model of the sensors system integration algorithm.

misalignment of the input axis with respect to the output axis, cross-axis sensitivity, noise and erroneous calibration of the scale factor. This accelerometer model is obtained using the following equation [25–27]:

$$a_s = E/K_1 = K_o + a_i + K_2 a_i^2 + K_3 a_i^3 + K_{ip} a_i a_p + K_{io} a_i a_o + \delta_o a_p - \delta_p a_o + v, \tag{9}$$

where a_s is the acceleration indicated by the accelerometer, E - sensor output, K_1 - scale factor, K_o - bias, K_2, K_3 - second-order, respectively third-order, nonlinearity coefficients, K_{ip}, K_{io} - cross-coupling coefficients, δ_o, δ_p - misalignments of the input axis with respect to the input reference axis about the output reference and pendulous reference axes, respectively, a_i, a_p, a_o - applied acceleration components along the positive input, pendulous, and reference axes, respectively, and v - sensor's noise.

3.2. Matlab/Simulink Models for Accelerometers

Most of the numerical simulations for the inertial navigation systems, from different bibliographical research, assume the inputs expressed in terms of clean angular speed and acceleration signals, without noises and errors. Then, the full errors studies for the inertial systems are usually done without taking into account the sensors errors. In order to realize a complex study for the navigation systems, close to real conditions (which includes the real errors of the used sensors), an acceleration sensors model can be conceived and equivalent with the model described by Eq. (9). The conceived model should consider the parameters provided by the data sheets offered by the producers. Therefore, following a detailed study of the data sheets for a series of accelerometers [6, 13–17], a simplified model is obtained, which covers the main errors of the accelerometers, that cannot be directly compensated:

$$a = (a_i + N a_i + B + k_c a_c + v)(1 + \Delta K/K), \tag{10}$$

where a is the output acceleration (perturbed signal), a_i - input acceleration, N - misalignment of the sensitive axis, B - bias, a_c - cross-axis acceleration, k_c - cross-axis sensitivity, v - sensor noise, K - scale factor, and ΔK - the scale factor calibration error. The model quantities, and their respective units are expressed in Eq. (10) as follows: accelerations a, a_i and a_c in m/s^2, N in radians, B in percents of span, k_c in percents of a_c, K in mV/g, ΔK in percents of K, and the noise v is given through its density v_d expressed in μg/Hz$^{1/2}$.

Considering this analytical simplified model, we obtained a Matlab/Simulink model, generally valid for the acceleration sensors, based on the accelerometer parameters variation limits, provided by the data sheets (Fig. 4). In the model, is observed that a part of the sensors parameters given in the data sheets do not have a fixed value and vary arbitrarily in an interval.

In this way, the bias is given through its maximum absolute value B as the span percentage, the cross-axis sensitivity is given through its maximum value k_c as an acceleration a_c percentage, the scale factor calibration error is provided through its maximum absolute value ΔK as a percentage of scale factor K and the noise is given through its density maximum value.

The bias are generated as random values in the $(-B, B)$ interval, the cross-axis sensitivity in the $(0, k_c)$ interval and the scale factor calibration error in the $(-\Delta K, \Delta K)$ interval, using the Matlab function ''rand(1)''. The noises are generated using the Simulink block ''Band-Limited White Noise'' and the Matlab function ''RandSeed'' through the random selection of its density value in the $(80\% \cdot v_d, v_d)$ interval.

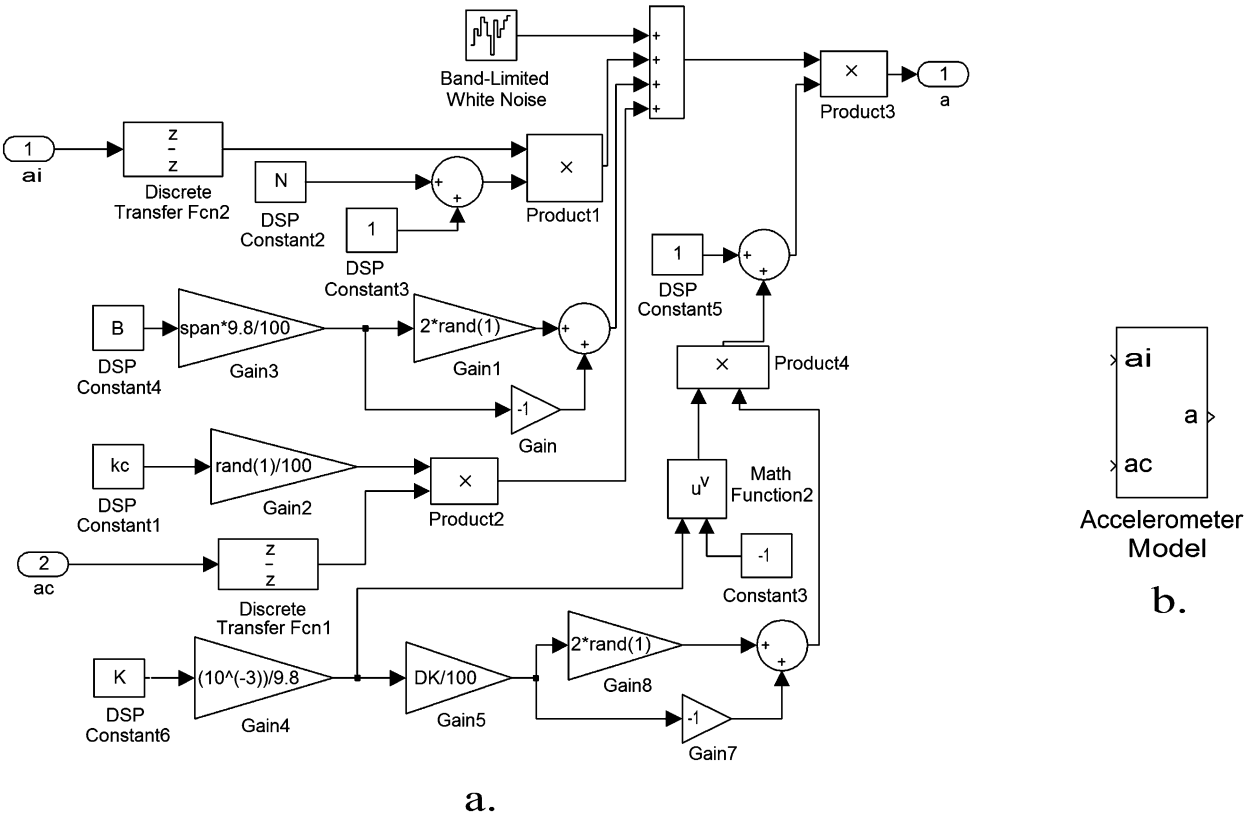

Fig. 4. Matlab / Simulink accelerometers model.

The block shown in Fig. 4(b) summarized the scheme composed of different blocks shown in Fig. 4(a). This block has two inputs: the acceleration a_i applied along of the sensitive axis, and the cross-axis acceleration a_c. Its output is the perturbed acceleration a.

The accelerometers model was built for few acceleration sensors, using the MEMS or MOEMS technologies or the classical approach. The change of the sensor type is done using the interface shown in Fig. 5. In addition, this interface allows the model setting, by the user, in a custom variant, with the parameters manual insertion in the characteristic fields. Because of the custom variant, the model may consider separately with each of the sensors errors – and in this way, the impact of each sensor errors is evaluated in the navigation system final errors.

4. RESULTS

In the first phase, the algorithm testing is realized by consideration of the noise overlapped on the useful signal. Because of the custom variant, the accelerations sensors model previously created, allows now the setting of such a signal. In this way, a MOEMS accelerometer model was used for numerical simulations. Its characteristics are: the acceleration range $\pm$ 20 g, the scale factor 50 mV/g, the bandwidth 100 Hz, the noise density 120 $\mu g/Hz^{1/2}$, the bias 2% of span, the scale factor error 5% of scale factor, the cross-axis sensitivity 3%, and the misalignment of the sensitive axis of 0.01 radians. Thus, if four accelerometers would be fixed on the same axis ($n = 4$), with the input (a_i) and the cross-axis accelerations (a_c) nulls, respectively, the simulation model leads to the graphical characteristics shown in Fig. 6.

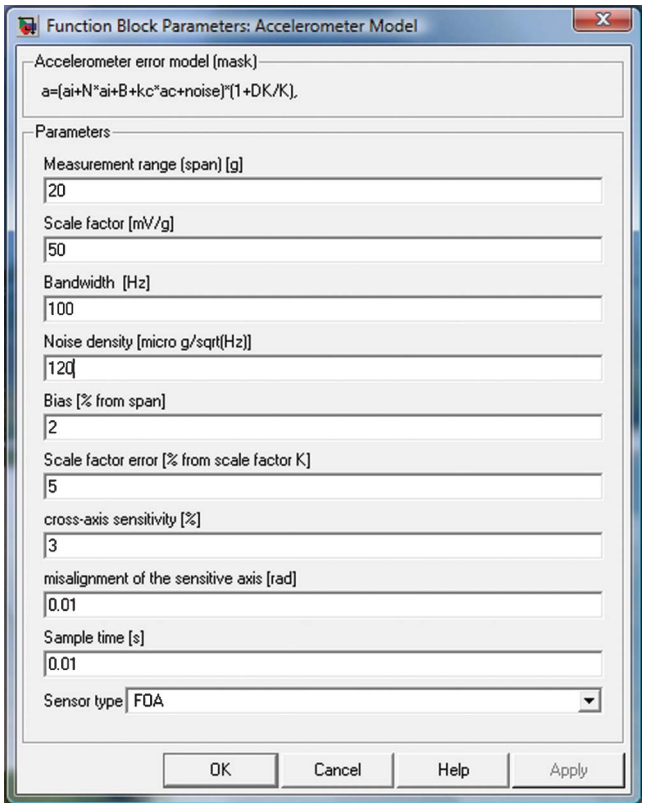

Fig. 5. The parameters setting for the accelerometers error model.

In Fig. 6, the signal obtained through the application of the integration algorithm (a_{IA}) for the four sensors was plotted with thick line, while the sensors outputs ($a_{sensors}$) perturbed by noise if they work independently were plotted with narrow lines. It could be observed that the resultant signal passes through values located between the values corresponding to the four accelerometers at the same time, nearly to the most accurate accelerometer in that area. The resultant signal was found to be less affected by the noise with respect to the four accelerometers output signals. We conclude that the algorithm works correctly, as it gives the highest weight, in the final acceleration calculus, to the most accurate accelerometer.

In case when the same conditions would be considered for the numerical simulation of the integration algorithm, for different number n of the sensors set on the input axis of the strap-down inertial navigation system (n=1, 2, 5, 10, 20, 25, 50, 100), then the output signals of the integrated system for all studied cases are shown in Fig. 7.

For the input acceleration a_i of 10g, and same n values, the graphical results are shown in Fig. 8. For a ramp a_i signal with the value $5{\cdot}10^{-4}$g after a time of 10 seconds, for the first second, the graphical characteristics are shown in Fig. 9. For the numerical simulations, the number of samples in the buffer m=100 is considered.

Following the analysis of graphical results, it is observed a rapid noise decrease simultaneously with the increase of the acceleration sensors number set on the input axis. The estimation of the algorithm performances from the noise reduction point of view is realized by calculating the ratio between the medium power spectral density at the input, for n accelerometers, and the signal power spectral density obtained at the integrated system output. The signal power spectral density, including its noise was determined with the ''PSD'' Matlab function.

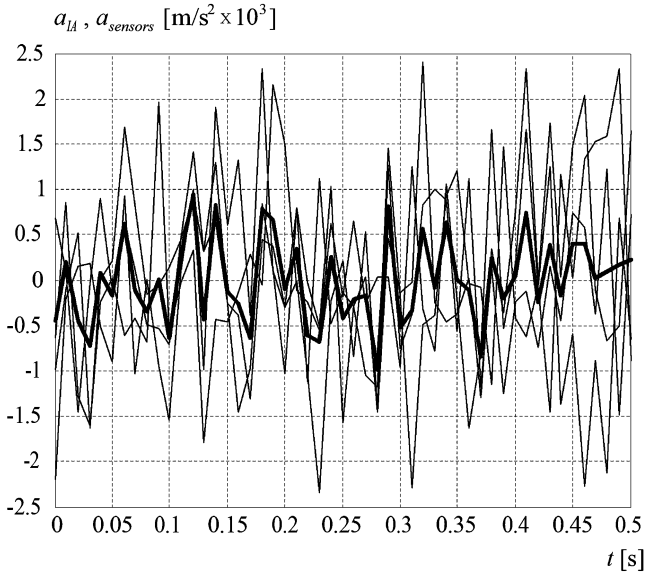

Fig. 6. Outputs of the integration model and of the four accelerometers.

In Table 1, the maximum deviation of the output signal from the real value applied on the input and the decreasing ratio of the power spectral density for all n studied values are shown for all three cases. The numerical results confirm the noise reduction. The reduction of the noise

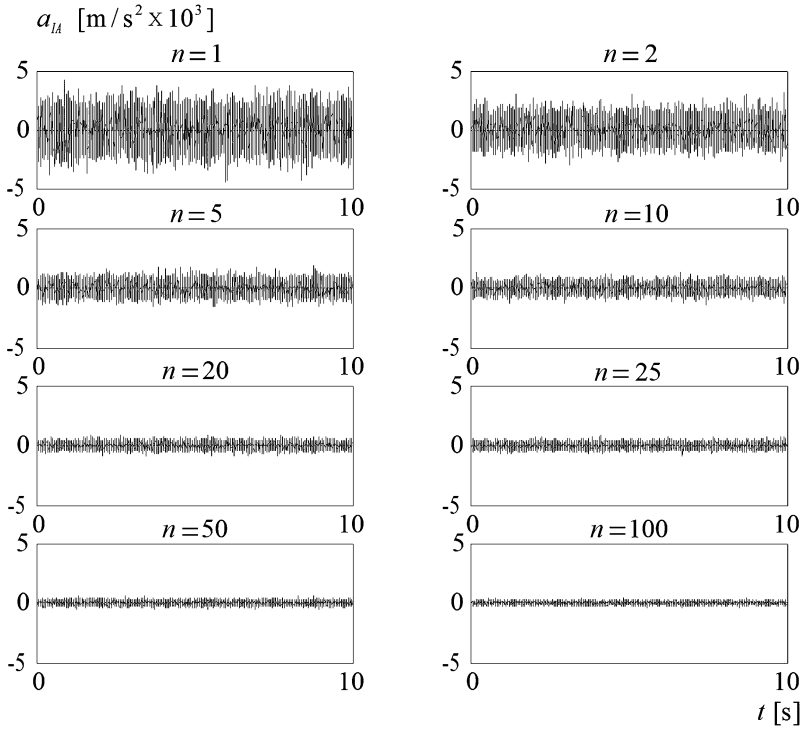

Fig. 7. $a_{IA}(t)$ for a_i=0g and different n.

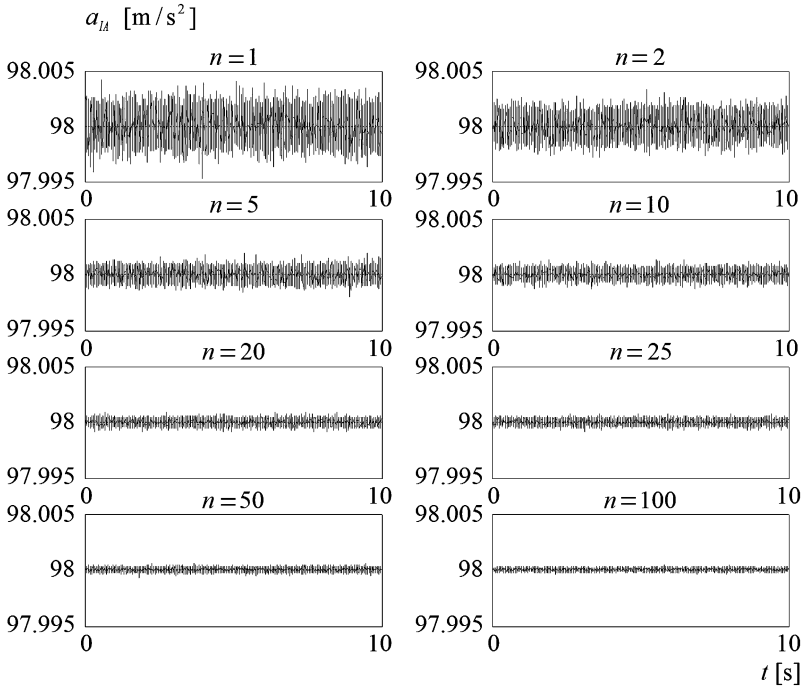

Fig. 8. $a_{IA}(t)$ for a_i=10g and different n.

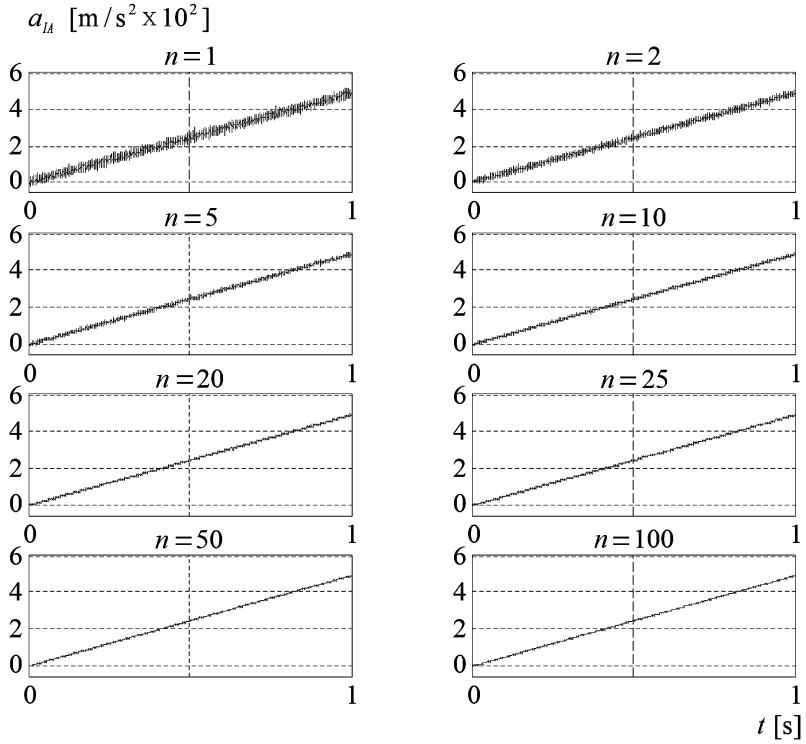

Fig. 9. $a_{IA}(t)$ for a_i - ramp and different n.

Table 1. The maximum deviation of the output signal from the real value applied on the input and the decreasing ratio of the power spectral density.

Sensors number n	a_i = 0 g		a_i = 10 g		a_i - ramp signal	
	Ratio	deviation [m/s^2]	Ratio	deviation [m/s^2]	Ratio	deviation [m/s^2]
1	-	0.00415	-	0.00414	-	0.00462
2	1.9621	0.0031	1.9706	0.0033	2.0319	0.00308
5	5.0194	0.00185	5.0732	0.00188	5.0865	0.00177
10	10.1478	0.00129	10.4373	0.00137	9.5928	0.00123
20	19.5428	0.00087	18.8548	0.00088	19.349	0.00106
25	25.8728	0.0008	25.5586	0.00073	25.4343	0.00094
50	50.1117	0.00063	50.1932	0.00061	52.5028	0.00067
100	102.9608	0.00039	101.6118	0.00048	103.6518	0.00043

power spectral density for the output signals of the n sensors integrated system is proportionally with the sensors number. We conclude that the noise density would be reduced direct proportionally with $n^{1/2}$.

The second testing algorithm phase considers all errors appearing in the accelerometers models. Using five accelerometers on the input axis (n=5), for null input (a_i=0g) and for a cross-axis acceleration a_c=1g, the numerical simulation of the Matlab/Simulink model in the integration algorithm leads to the graphical characteristics shown in Fig. 10.

The obtained characteristics show the perturbed outputs of the five sensors and the output acceleration signal from the integrated system, respectively in Fig. 10. It can be observed that the bias has a very important influence on the individual signals obtained from the

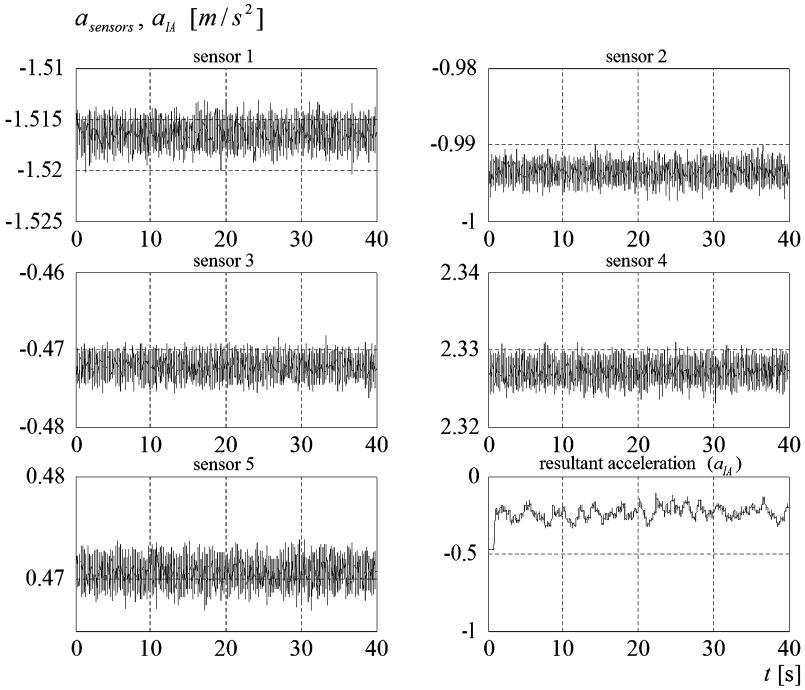

Fig. 10. a_{sensors} and $a_{IA}(t)$ for a_c=1g with real model.

accelerometers. As the sensors category is the same, the bias can take a random value in $(-B, B)$ interval, and then the output signal obtained through the sensors integration would have a mean value near zero. The mean value of the resulted signal is obtained through the averaging of the integrated sensors biases.

The overlapping of the noises and of others errors, which could take random values between certain limits for a category of integrated sensors, generates a signal with a reduced noise, which has the tendency to oscillate around a value so much near to the non-perturbed input signal a_i, as higher the sensors number is. An interval of approximately 1 second at the beginning of the simulation, it can be observed on its lower right part of Fig. 10. The explanation is that the number of samples for which the standard deviation is calculated, and which increases from $m=1$ to $m=100$, at which the algorithm is set.

The acceleration characteristics are shown in Fig. 11, by considering the step input signal $a_i=1$g, the cross-axis acceleration $a_c=1$g and four integrated acceleration sensors ($n=4$). The output signal of the integrated system is shown by thick line, and the non-perturbed input is shown with narrow line. The other graphical characteristics represent the perturbed outputs of the accelerometers used in the algorithm. There are big differences between the accelerometers outputs and their non-perturbed input, due to their biases. Because of the high values of the depicted signals means, the noise affecting them is less visible in the figures. It can be easily observed the same tendency of the output acceleration oscillation near the non-perturbed input.

A very fast a_i signal (Fig. 12), of repeated ramp type, characterized by strongly jumps from the positive to negative values and inversely, is applied at the sensors input; this input is presented with narrow line. For a number of four accelerometers ($n=4$) subjected to the cross-axis acceleration $a_c=1$g, the acceleration characteristics are given in Fig. 13. The resultant acceleration is drawn with thick line in both Figs. 12 and 13. The signal obtained through the sensors system integration, shown in Fig. 12, follows the input signal, but with a deviation equal with the mean of the algebraically values of the four accelerometers' biases.

By comparison of the curves shapes describing the perturbed outputs of each of the four accelerometers and the curve shape showing the resultant acceleration a_{IA} (represented with

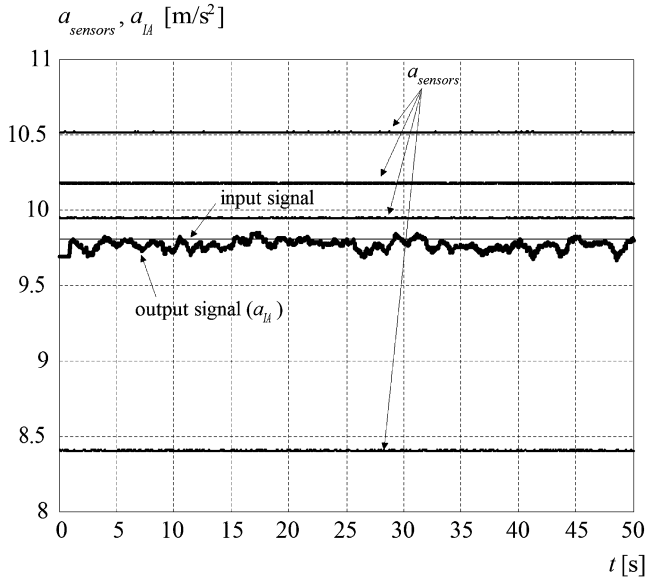

Fig. 11. a_{sensors} and $a_{IA}(t)$ at $a_i=1$g and $a_c=1$g with real model.

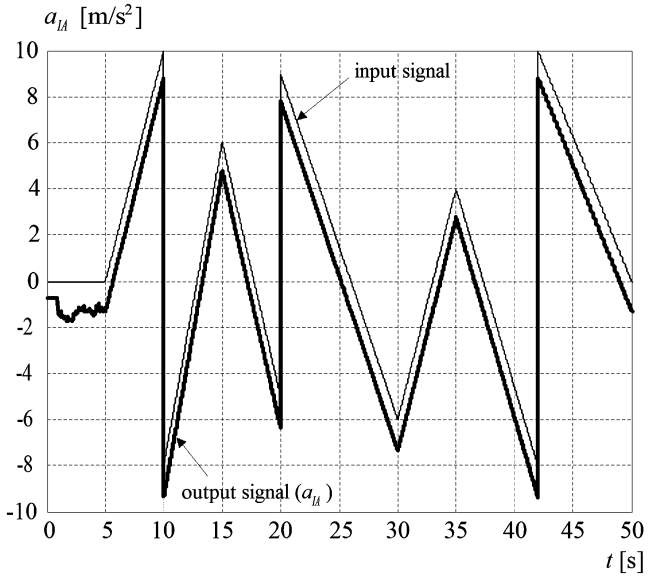

Fig. 12. $a_{IA}(t)$ at a_i variable in time.

thick line) in Fig. 13, it can be observed that very good results are obtained using our algorithm - and fast signals are given as inputs. The output of the integrated system is much closer to the signal obtained for the most accurate accelerometer with the highest calculus weight. As in previous cases, the output signal is on an interval of approximately 1 second, where the algorithm starts. In the intervals with constant input acceleration, the output signal has the tendency to oscillate near by this input, but with a deviation equal with the mean of the integrated sensors biases algebraically values.

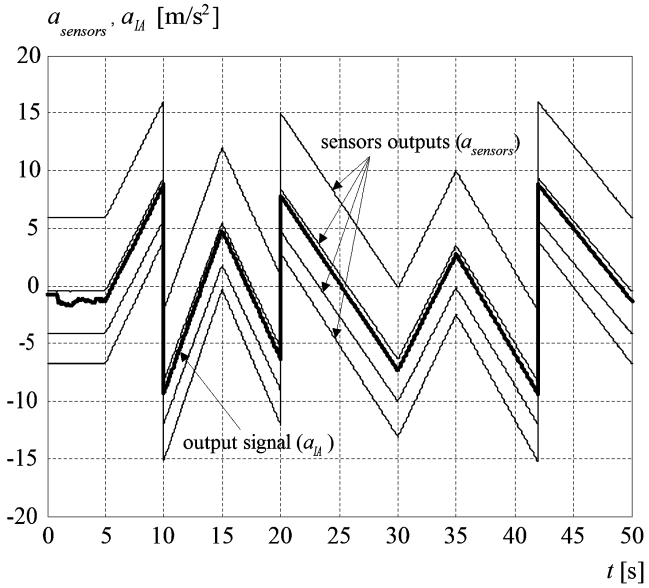

Fig. 13. a_{sensors} and $a_{IA}(t)$ at a_i variable in time.

5. CONCLUSIONS

The numerical simulations results confirm the obtaining of an integration algorithm for the miniaturized inertial sensors, based on the setting on the same axis of a high number of sensors, of the same type. This algorithm reduces the signal noise power delivered to the navigation processor, proportionally with the integrated sensors number. At the same time, the algorithm reduces the bias of the resulted signal, by averaging the algebraically values of the integrated sensors biases. A high redundancy degree for the strap-down inertial navigation system at a low-cost with respect to more accurate and expensive sensors is also provided.

It could be concluded that an optimal value for the number of the sensors set on the input axis should be $n = 5$, when the noise density would be reduced by 2.23 times. The doubling of the sensors number ($n = 10$) is not justified for a reduction by 3.16 times of the noise density, for an inertial navigation system used in applications which do not require a special accuracy. The number of the sensors can be increased to 100 in high accuracy applications, because the actual technology allows these conceptions in a single chip, including the afferent circuits for supplying and for the signals conditioning. In this case, a ten (10) time reduction of the noise density is obtained.

REFERENCES

1. Grigorie, T.L., *Sisteme de navigatie inertiala strap-down. Studii de optimizare*, Editura SITECH, Craiova, Romania, pp. 1–328, 2007, ISBN: 978-973-746-723-2.
2. Lungu, R. and Grigorie, T.L., *Traductoare Accelerometrice si Girometrice*, Editura SITECH, Craiova, Romania, pp. 1–206, 2005, ISBN: 973-657-777-5.
3. Grigorie, T.L. and Botez, R.M., "The bias temperature dependence estimation and compensation for an accelerometer by use of the neuro-fuzzy techniques," *Transactions of the Canadian Society of the Mechanical Engineering (CSME)*, Vol. 32, No. 3, pp. 383–400, 2008.
4. Grigorie, T.L., Jula, N., Cepisca, C., Racuciu, C. and Raducanu, D., "Evaluation Method of the Sensors Errors in an Inertial Navigation System," *Wseas Transactions on Circuits and Systems*, Vol. 7, No. 12, pp. 977–987, 2008, ISSN: 1109-2734.
5. Grigorie, T.L., "Some considerations concerning the influence of the inertial sensors errors on the solution of navigation for a bidimensional strap-down inertial navigation system," *5th IEEE Workshop on Positioning, Navigation and Communication 2008 (WPNC'08)*, Hannover, Germany, pp. 149–156, March 27, 2008.
6. MSISensors webpage <http://www.msisensors.com>
7. Lawrence, A., *Modern inertial technology: navigation, guidance and control*. Springer Verlag, New York, 1993.
8. Barbour, N. and Schmidt, G., "Inertial Sensor Technology Trends,"*IEEE Sensors Journal*, Vol. I, No. 4, pp. 332–339, December 2001.
9. Maenaka, K., "MEMS Inertial Sensors and Their Applications," *5th International Conference on Networked Sensing Systems*, Kanazawa, Japan, June 17–19, 2008.
10. Radix, J.C., *Systemes inertiels a composants lies <<Strap-Down>>*, Cepadues-Editions, Ecole Nationale Superieure de l'Aeronautique et de l'Espace SUP'AERO, Toulouse, 1993.
11. Grigorie, T.L., Sandu, D.G. and Aron, I., "Redundancy achievement and accelerometer's noise reduction in low-cost strap-down inertial navigation systems," *AIAA International Conference on Nonlinear Problems in Aviation and Aerospace ICNPAA 2006*, Budapest, Hungary, June 21–23, 2006.
12. Varadan, V.K. and Josek, K.A., "Wireless navigation inertial sensors on a single chip with Bluetooth Technology," *Proceedings of Electronics and Structures for MEMS II Conference*, Adelaide, Australia, pp. 266–272, December 17–19, 2001.

13. Analog Devices webpage: <http://www.analog.com>
14. Crossbow Technology webpage <http://www.xbow.com>
15. Honeywell Avionics webpage <http://www.honeywell.com/sites/aero/technology/avionics.htm>
16. Phone-or webpage <http://www.phone-or.com>
17. Silicon Designs webpage <http://www.silicondesigns.com>
18. Grigorie, T.L., Hiliuta, A., Botez, R.M. and Aron, I., "Étude numérique et expérimentale d'un algorithme d'attitude pour un système inertiel à composantes liés," *Transactions of the Canadian Society of the Mechanical Engineering (CSME)*, Vol. 30, No. 3, pp. 429–442, 2006.
19. Grigorie, T.L., "The Matlab/Simulink modeling and numerical simulation of an analogue capacitive micro-accelerometer. Part 2: Closed loop," *The IEEE 4nd International Conference on Perspective Technologies and Methods in MEMS Design*, Polyana, Ukraine, pp. 115–121, mai 21 - 24, 2008.
20. Grigorie, T.L., "The mathematical modeling and numerical simulation of an open loop analogue capacitive micro-accelerometer," *AIAA/IEEE 12th Saint Petersburg International Conference on Integrated Navigation Systems*, Saint Petersburg, Russia, May 23–25, 2005.
21. Grigorie, T.L., "An optimization procedure for a fiber optic accelerometer," *The IEEE 3nd International Conference on Perspective Technologies and Methods in MEMS Design*, Polyana, Ukraine, pp. 15–19, 23 - 26 may, 2007.
22. Cui, J., Falconer, D.D and Shreikh, A.U.H., "Performance evaluation of optimum combining and maximal ratio combining in the presence of co-channel interference and channel correlation for wireless communication systems," *Mobile Networks and Applications*, Vol. 2, pp. 315–324, 1997.
23. Chen, Z., Yuan, J. and Vucetic, B., "Analysis of Transit Antenna Selection/Maximal-Ratio Combining in Rayleigh Fading Channels," *IEEE Transactions on Vehicular Technology*, Vol. 54, No. 4, pp. 1312–1321, July 2005.
24. Tomiuk, B.R. and Beaulieu, N.C., "A new look at maximal ratio combining," *IEEE Global Telecommunications Conference GLOBECOM'00*, San Francisco, USA, pp. 943–948, 27 November–1 December 2000.
25. IEEE Std. 528-2001, *IEEE Standard for Inertial Sensor Terminology*, Published by IEEE, New York, USA, 29 November, 2001.
26. IEEE Std. 1293-1998, *IEEE Standard Specification Format Guide and Test Procedure for Linear, Single-Axis, Nongyroscopic Accelerometers*, Published by IEEE, New York, USA, 16 April, 1999.
27. IEEE Std. 836-1991, *IEEE Recommended Practice for Precision Centrifuge Testing of Linear Accelerometers*, Published by IEEE, New York, USA, June 15, 1992.